RJC

RASĀYAN *J. Chem.*
Vol. 18 | No. 4 |2012-2019| October-December | 2025
ISSN: 0974-1496 | e-ISSN: 0976-0083 | CODEN: RJCABP
http://www.rasayanjournal.com
http://www.rasayanjournal.co.in

UTILIZATION OF CRAB SHELLS (*Portunus pelagicus Linn*) AS A BASE MATERIAL FOR SELECTIVE ADSORBENT OF Ni(II) AND Zn(II) IONS IN SEAWATER MEDIUM

M. Sehol[1,✉], K. Kasmawati[1], N. Narsito[2], S.J. Santosa[2], J. Jumina[2], R. Sholehah[3], Z.D. Firdaus[3], M. Mahfud[3], M.A. Ardiputra[4] and B. Sardi[5]

[1]Department of Biology Education, Iqra Buru University, Buru-97571, Indonesia
[2]Department of Chemistry, Gadjah Mada University, Sleman-55281, Indonesia
[3]Department of Chemical Engineering, Sepuluh Nopember Institute of Technology, Surabaya 60111, Indonesia
[4]Department of Biology, Tadulako University, Palu-94118, Indonesia
[5]Research Centre for Energy Materials, National Research and Innovation Agency, South Tangerang-15314, Indonesia
✉Corresponding author: lasehol@gmail.com

ABSTRACT

This study systematically investigates the utilization of crab shell waste (Portunus pelagicus Linn) as a basic material for selective adsorbents of Ni(II) and Zn(II) metals in a seawater medium. The process began with the isolation of chitin and chitosan through the stages of deproteinization, demineralization, and deacetylation, followed by the optimization of reaction conditions by varying the concentrations of HCl and NaOH, temperature, and reflux time. The optimized chitosan product was converted into chitosan beads and several chitosan derivatives, which were then tested as heavy metal adsorbents using batch and solid-phase extraction (SPE) systems. The results showed that increasing the concentration of NaOH, temperature, and reflux time affected the degree of deacetylation of chitosan. The optimum adsorption process occurred at pH 5–6, with a mechanism dominated by chemisorption based on desorption efficiency and the stability of the adsorbent against variations in pH and salinity. Chitosan and its derivatives demonstrated high selectivity and could concentrate Ni(II) and Zn(II) metals from µg/L levels to mg/L in the SPE system. Additionally, the flow rate and HCl concentration as the eluent had an impact on the adsorption-desorption efficiency. Overall, this study showed that crab shell chitosan derivatives had great potential as stable and selective adsorbents for applications involving the separation of heavy metals in marine environments.

Keywords: Chitosan Derivative, Heavy Metals, Marine Environment, Selective Adsorbent, Solid Phase Extraction.
RASĀYAN *J. Chem.*, Vol. 18, No. 4, 2025

INTRODUCTION

Heavy metal pollution in waters, especially in marine waters, is a very important environmental issue worldwide that requires special attention due to its effects on human health and ecosystems. Although heavy metals such as zinc (Zn) and nickel (Ni) are often found in low concentrations (µg/L) in seawater, they are still dangerous when accumulated.[1] However, heavy metal detection methods such as AAS or spectrophotometry remain generally limited to detection at the mg/L level, which necessitates reliable and economical preconcentration techniques.[2] One promising solution is the solid phase extraction (SPE) technique, which relies on adsorption using natural materials that have been chemically modified. Crab shells (*Portunus pelagicus Linn*), which are rich in chitin, have the potential to develop into chitosan-based adsorbents with active functional groups focused on certain heavy metals.[3] Several studies have shown that modifications to chitosan, such as the addition of glutaraldehyde groups, thiols, and phosphates, enhance the adsorption capacity and preference for metal ions. For example, Sutirman et al.,[4] found that at neutral pH, porous chitin cross-linked with poly(ethylene imine) showed different levels of preference for heavy metals. However, there are still some unresolved issues. Some of these include the instability of the binding groups that can detach during the adsorption-desorption process and poor selectivity towards target metals in complex matrices such as seawater.[5,6]

http://doi.org/10.31788/RJC.2025.1849396

In this situation, using crab shell chitosan as the preferred adsorbent for Ni(II) and Zn(II) metals becomes crucial, particularly in SPE systems that enable efficient reuse.[7] Research has so far only employed crab shell chitosan derivatives as adsorbents for Ni(II) and Zn(II) in complex seawater media. This research primarily uses the Hard-Soft Acid Base (HSAB) method. There are no systematic reports that combine the preparation of adsorbents, selectivity evaluation towards target metals, the main components of seawater, and applications in SPE columns.[8] As a result, this research offers a new approach by creating adsorbents derived from chitin modified with active groups such as glutaraldehyde and thiourea. The chemical properties of this adsorbent work with heavy metals. This discovery aims to address the issue of selectivity in seawater adsorption and opens up new opportunities for the use of marine biomass waste in water purification technology.[9]

In this situation, using crab shell chitosan as the preferred adsorbent for Ni(II) and Zn(II) metals becomes crucial, particularly in SPE systems that enable efficient reuse.[7] Research has so far only employed crab shell chitosan derivatives as adsorbents for Ni(II) and Zn(II) in complex seawater media. This research primarily uses the Hard-Soft Acid Base (HSAB) method. There are no systematic reports that combine the preparation of adsorbents, selectivity evaluation towards target metals, the main components of seawater, and applications in SPE columns.[8] As a result, this research offers a new approach by creating adsorbents derived from chitin modified with active groups such as glutaraldehyde and thiourea. The chemical properties of this adsorbent work with heavy metals. This discovery aims to address the issue of selectivity in seawater adsorption and opens up new opportunities for the use of marine biomass waste in water purification technology.[9]

EXPERIMENTAL

Equipment and Setup Experiment

This research used crab shells as the main adsorbent material. The material preparation process was carried out in an environmental chemistry laboratory, with the main equipment including a hotplate stirrer, water bath, drying oven, Fourier Transform Infrared Spectrophotometer (FTIR), and UV-Vis Spectrophotometer. Additional equipment included a pH meter, analytical balance, orbital shaker, and SPE column. The crab shells were washed thoroughly, dried, and then ground to a uniform size (<100 mesh). The series of adsorption experiments involved an SPE column filled with 0.1 g of adsorbent, a solution of Ni(II) and Zn(II) metals at 100 ppm in artificial seawater, and variations in pH, contact time, and leaching concentration (HCl) as testing variables.

Strategy and Analysis

Based on the modification of the method by Iber *et al.,*[10] the preparation of the adsorbent began with three main stages. Deproteinization was carried out with a 3.5% (w/v) NaOH solution for two hours at 65℃; demineralization was performed with 1 M HCl for 30 min at 60℃; and deacetylation was conducted with 50% NaOH for 30 min at 100℃. The resulting product was oven-dried at 60℃ until completely dry. Characterization of functional groups was performed using IR spectroscopy with the KBr pellet method. For the adsorption capacity test, Ni(II) and Zn(II) metal solutions were prepared with an initial concentration of 100 ppm. Every 10 mL of the solution was tested with 0.1 g of adsorbent in a shaker for 60–90 min at various pH levels (3–7), then filtered and analyzed using UV-Vis. Efficiency was calculated using the formula in eqn.-1.[11]

$$Adsorption(\%) = \left(\frac{C_O - C_f}{C_O}\right) \text{ x } 100 \qquad (1)$$

Where C_o = initial concentration and C_f = final concentration.

Conversion of Chitin-Chitosan from Crab Shells

Dried crab shells that had been ground and sieved to a 100 mesh size were processed into chitosan through three stages: deproteinization, demineralization, and deacetylation, based on the method by Fitriyana *et al.*[12] The deproteinization process was done by refluxing 90 g of shell powder in 900 mL of 3.5% NaOH for two hours at 65℃, then washing it until it was free of H^+ ions. The residue was then demineralized with 900 mL of 1 M HCl for 30 min at room temperature, filtered, washed until neutral, and dried at 60℃. For evaluation, the order of the process was also reversed to compare its effects. The final deacetylation stage was performed by refluxing 40 g of powder from the previous two stages in 400 mL of 50% NaOH at 100℃ for

30 min; the residue was then washed until neutral and dried. The product attained is chitosan powder that was derived from deacetylating crab shells.

Characterization of the Adsorbent using FTIR and XRD

The functional groups and the degree of deacetylation (DD) were calculated through IR spectroscopy on the crab shell powder, which Boulaiche *et al*.,[7] modified using a logic-enhancing spectrum baseline shift to get more reasonable outcomes. The analyzed samples included crab shells before and after the deproteinization, demineralization, and deacetylation stages, including products processed using the reversed sequence, as shown in Fig.-1. Each sample was mixed with KBr, pressed into pellets, and then analyzed using IR spectroscopy. The DD values from each spectrum were used to evaluate the success of chitin and chitosan conversion. In addition, crystal structure characterization was performed using a Siemens D5005 X-ray diffractometer to observe changes in the degree of structural order resulting from the treatment of crab shells.[13,14]

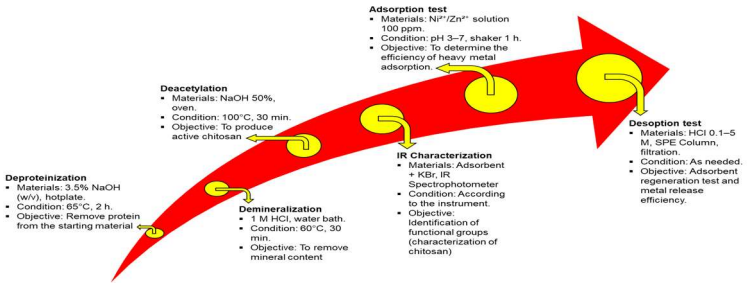

Fig.-1: Adsorbent Characterization Process Using FTIR and XRD

Testing the Adsorption of Ni(II) and Zn(II) Metals in Seawater Medium

Chitosan was synthesized from crab shells through a demineralization process using HCl (0.2–1 M) and deacetylation with NaOH (50–70%) at various temperatures and durations, which resulted in a high-quality adsorbent. To identify the functional groups and determine the degree of deacetylation, the synthesized chitosan was analyzed using infrared spectroscopy. Then, the synthesized adsorbent was tested for its ability to adsorb Ni(II) and Zn(II) metals from a 100 ppm metal solution under various conditions, including pH (2–10) and contact time (30–1380 min), as well as in a seawater medium. The adsorbent-metal solution mixture was shaken and filtered. Using UV-Vis spectroscopy and atomic absorption spectroscopy (AAS), the difference between the initial and residual metal concentrations was measured to estimate adsorption. This evaluation was used to compare the adsorptive capacity of chitosan under different synthesis and environmental conditions.[15]

Experiment on Selectivity and Desorption

Chitosan was chemically modified by the reaction of several compounds in acetic acid with glutaraldehyde, thiourea, thiocyanate, sulfate, molybdate, and chitosan phosphate. The resultant solution was neutralized with NaOH, and the precipitate obtained was dried. The absorbent, either as a powder or granules, was analyzed using XRD and IR spectroscopy. The ability of the synthesized absorbent to adsorb Zn(II) and Ni(II) ions was also investigated. The competitive selectivity test is done using Ni(I) ions added to a solution with Zn(I) to observe how other ions in the solution affect adsorption effectiveness. Subsequently, desorption tests were carried out by dissolving the adsorbed metals using HCl at various concentrations (0.1–5 M), to evaluate the strength of interaction between the metals and the adsorbent, as well as assess the regeneration potential of the chitosan-derived materials.

RESULTS AND DISCUSSION

Conversion of Chitin to Chitosan

The preparation process of crab shells involved the stages of deproteinization, demineralization, and deacetylation, which resulted in adsorbents with enhanced structure and surface properties. IR spectra showed the presence of key functional groups such as –OH, –CH methylene, and –C=O carbonyl, as well as the presence of SiO_2 identified from characteristic absorption bands in the spectrum, indicating resistance to degradation during the chemical process.[16] Following demineralization and deacetylation, the X-ray

diffractogram displayed an increase in crystalline intensity, signifying that the adsorbent structure had been successfully modified. A high degree of chitosanization and the ability to bind heavy metal ions were indicated by the DD value, which was 70.63%. According to the adsorption results, monolayer adsorption on the adsorbent surface was supported by the significant adsorption of Ni(II) and Zn(II) metals at an optimal pH of 5–6 with a Langmuir isotherm pattern.[17]

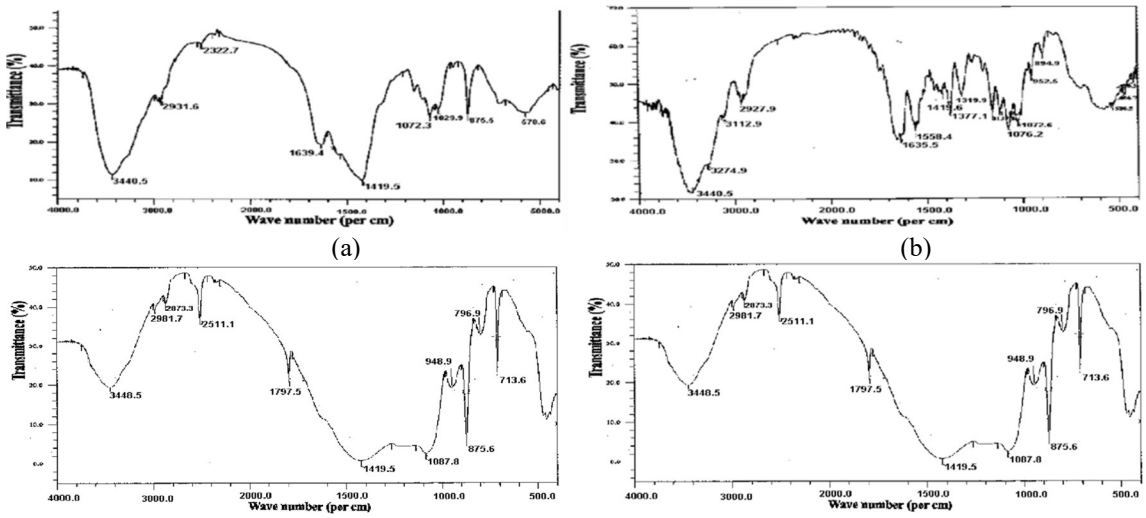

Fig.-2: IR Spectrum of Crab Shell: (a) Raw Material; (b) Demineralized at –C=O Carbonyl; (c) Demineralized at SiO_2–$CaCO_3$; (d) Deacetylated

Figure-2(a) and Fig.-2(b) show the IR spectra before and after treatment, displaying intensified –OH and –C=O group intensities post-deacetylation. Figure-2(c) and Fig.-2(d) showed X-ray diffractograms with sharper intensity peaks on the deacetylated adsorbent, indicating an increase in crystallinity. The processes of deproteinization, demineralization, and deacetylation were carried out sequentially to remove proteins and metal impurities from the crab shell. It was clear from the IR spectra that the bands at 2931.6 cm^{-1} (Fig.-2(a)) and 2927.7 cm^{-1} (Fig.-2(b)) represented the symmetric stretching vibration of –CH_2–, while the absorption bands at 3440.8 cm^{-1} (Fig.-2(a)) and 3448.5 cm^{-1} (Fig.-2(b)) indicated the presence of –OH groups.[3] The absorption bands at 1639.4 cm^{-1} (Fig.-2(c)) and 1635.5 cm^{-1} (Fig.-2(b)) indicated the presence of the –C=O carbonyl group from acetamide, and the band at 1419.5 cm^{-1} that appeared in all images indicated the presence of the –C=O carbonate group from $CaCO_3$. Additionally, the bands at 1072.5 cm^{-1} and 1076.2 cm^{-1} (Fig.-2(a) and Fig.-2(b)) as well as 952.6 cm^{-1} (Fig.-2(b)) showed the presence of silicon metal impurities in the form of SiO_2. Thus, the IR spectrum of the SiO_2–$CaCO_3$ (1:1) mixture (Fig.-2(c)) confirmed the presence of carbonate and silicate groups, indicating that silicon metal was very difficult to remove through the demineralization process. This was demonstrated by the characteristic absorption bands at 1419.5; 1087.8; and 948.9 cm^{-1} that also appeared in the demineralized shell spectrum (Fig.-2(c)). In the final stage, the deacetylation process using high-concentration NaOH produced the IR spectrum of the deacetylated shell (Fig.-2(d)), which showed a decrease in the intensity of the 1639.4 cm^{-1} band, indicating the degradation of the carbonyl group from acetamide. However, the carbonate band at 1419.5 cm^{-1} remained, indicating that $CaCO_3$ had not been eliminated. Additionally, the bands at 1072.5; 1076.2; and 952.6 cm^{-1} still appeared in Fig.-2(d), confirming that neither demineralization nor deacetylation was effective in removing silica impurities (SiO_2). Additional data from the X-ray diffractogram in Fig.-2(c) showed that the demineralized shell had higher intensity peaks compared to the deacetylated shell, indicating higher crystallinity. These findings were consistent with the research results of Frenchibai *et al.*,[18] and Chang *et al.,*[19] and supported the success of the crab shell preparation process according to the designed stages.

The Connection between Nitrogen Content and DD Value

Table-1 compares nitrogen levels as a measure of the DD, which increased following deproteinization. In

general, the data shown in Table-1 indicate an increase in nitrogen content after chitin was converted into chitosan, both in terms of experimental results and theoretical calculations. From the data, the nitrogen content of chitosan calculated theoretically slightly differed from the experimental results (Kjeldahl method), but overall, the differences were not too significant, and some even showed relatively small value gaps. This fact indicated a correlation between the DD value and the nitrogen content calculated theoretically and confirmed by experimental data.[20]

Table-1: The Nitrogen Content is Based on Experimental and Theoretical Findings

Formula	Nitrogen (%)			
	Demineralized Crab Shell (Chitin)		Deacetylated Crab Shell (Chitosan)	
	Experiment	Calculation	Experiment	Calculation
1	4.99	4.99	7.10	6.00
2	4.99	4.99	7.10	5.67
3	4.99	4.99	7.10	-
4	4.99	4.99	7.10	6.21
5	4.99	4.99	7.10	5.98
6	4.99	4.99	7.10	5.53
7	4.99	4.99	7.10	6.20
8	4.99	4.99	7.10	5.85

The increase in nitrogen content along with the increase in DD was very relevant and quite realistic due to the release of several acetyl groups (–$COCH_3$) at the chitin acetamide sites, leaving amine groups (–NH_2) on the chitosan structure.[20]

The Adsorption Capacity of Chitin and Chitosan Towards Ni(II) or Zn(II) Metals

Table-2 showed the correlation between the DD and the adsorption capacity towards Ni(II) or Zn(II) ions, as an indicator of the ability of the –NH_2 group to bind metals.

Table-2: The Adsorption Capacity of Chitin and Chitosan Adsorbents in Adsorbing Ni(II) or Zn(II) Adsorbates.

Adsorbent	Degree of Deacetylation (%)	Adsorption Capacity of Ni(II) or Zn(II) (%)	Remarks		
			NaOH (%)	Refluks Time (min)	Temperature (°C)
A	47.00	11.40	30	30	100
B	53.00	21.70	40	120	120
C	75.60	27.00	50	30	100
D	82.40	31.00	50	120	100
E	91.00	39.40	50	1380	100
F	96.00	56.30	60	240	120

From Table-2, a correlational relationship was observed between the ability to adsorb Ni(II) or Zn(II) metals and the DD of chitin and chitosan. It appeared that the higher the degree of deacetylation of the chitosan adsorbent, the greater the increase in adsorption capacity for Ni(II) or Zn(II) metals. The increasing adsorption capacity for metal ions due to the influence of increased DD of the adsorbent showed quite significant linearity, as presented in Table-2. The increasing degree of deacetylation of chitosan allowed for the presence of more amine groups, which indirectly meant it also had a higher content of nitrogen atoms. The abundance of nitrogen atoms was what caused the high adsorption capacity for Ni(II) or Zn(II) metals, due to the increasing chelating ability as the degree of deacetylation of chitosan increased.[21]

The Adsorption Capacity of Phosphate Chitosan, Thiocyanate Chitosan, and Molybdate Chitosan Towards Ni(II) and Zn(II) Adsorbates

Table-3 presents the adsorption efficiency of Ni(II) and Zn(II) using various chitosan derivatives, showing that the bead form had the highest efficiency compared to the powder form. From the data presented in Table-3, it was generally shown that the new active sites generated from the interaction process between chitosan active sites and conversion solutions were capable of enhancing the adsorption capacity for Ni(II) metal. It also appeared that there was a slight improvement in adsorption capacity when the chitosan derivative adsorbent was used in the form of beads.

Table-3: Adsorption of Ni(II) by Several Chitosan-Derived Adsorbents

Adsorbents	Adsorption Capacity (%)
KFb	57.60
KFs	49.20
KTn	33.30
KMb	60.00
KMs	48.90
Ks	32.00

The IR spectra of phosphate chitosan (KFs and KFb) before and after interaction with Ni(II) showed changes in the absorption bands around the 1600–1500 cm^{-1} region. In that absorption region, the absorption intensity appeared to weaken somewhat after both adsorbents interacted with Ni(II). This indicated the occurrence of an adsorption process between Ni(II) metal and the main active sites, resulting from the conversion previously identified around the adsorption area. The appearance of a sharp absorption band in the 1380 cm^{-1} region also supported the adsorption process of Ni(II) by the KFs and KFb adsorbents. The fact that the absorption band around the 1380 cm^{-1} region in the IR spectrum of the chitosan phosphate adsorbents (KFs/KFb + Ni^{2+}) sharpened yielded results identical to the absorption band pattern observed during the adsorption process of Cu(II) by the chitosan adsorbent.[22] This indicated that both the active sites of chitosan and those of the KM and KMb adsorbents were capable of adsorbing Ni(II), resulting in IR spectra that differed from the IR spectrum of chitosan before conversion. This fact was reinforced by the spectral changes in the absorption region around 3400s–2800s, which initially showed prominent and broad spectra, but weakened during the adsorption process with Ni(II). There was a tendency that the presence of the –NH group from the $–NH_2$ group in chitosan, which possibly overlapped with the –OH group spectrum in the absorption region, experienced a change in absorption intensity after adsorbing Cu(II). Alternatively, the change in the absorption band was also caused by the role of the –OH groups present in both adsorbents (KMs and KMb) in adsorbing Ni(II).[23]

Surface Chemistry and Adsorption Performance

The presence of the -C=O amide functionality and the -OH hydroxyl group was impactful, as indicated by the IR spectrum. It was demonstrated that these functional groups were instrumental in the adsorption process of Ni(II) and Zn(II) metals through both electrostatic forces and coordination bond interactions. The Influence of Adsorption on pH reveals that the most favorable adsorption condition was at levels 5-6, which corresponds to the mildly acidic natural state of seawater. At lower pH levels, H^+ ions, along with the metals, competed for active site binding, while at higher pH levels, the metals precipitated out as hydroxides, which lowers adsorption efficacy.[22]

Adsorption Mechanism and Kinetics

Experimental procedures over adopting different analytic techniques revealed that the majority of the adsorption processes were completed within 30 min, achieving equilibrium after 90 min. This comported with the pseudo-second-order kinetic model, which fitted best, implying the process of adsorption was dominated by the chemical bond formation between the functional groups and the metal ions. The Langmuir isotherm model indicated that adsorption was monolayer in nature, with a maximum capacity of 42.5 mg/g for Ni(II) and 38.7 mg/g for Zn(II). The presence of amine groups ($–NH_2$) and newly introduced active groups such as –C=S in chitosan derivatives enhanced adsorption capacity, particularly toward borderline metals like Cu(II), by the Hard and Soft Acids and Bases (HSAB) theory.[24]

Implication and Selectivity Toward Ni(II) and Zn(II)

The amine functionalities of the carbonyl grouping, together with a crystalline structure, synergistically made the adsorbent more selective toward two metals, Ni(II) and Zn(II). Despite Cu(II) having stronger interactions and higher adsorption capacity, the results showed that crab shell-based adsorbents continued to perform well in seawater relative to the target metals. The influence of initial adsorbate concentration on adsorption capacity showed an increasing trend until a saturation point was reached, in accordance with the Langmuir isotherm model. This study demonstrated that adsorbents derived from crab shell waste possessed high potential as environmentally friendly and cost-effective alternatives for treating seawater contaminated with heavy metals.[24,25]

CONCLUSION

Using the shells of crab species Portunus pelagicus Lin as a source for biomaterials has precipitated great promise in removing heavy metals like Ni(II) and Zn(II) from seawater mediums. This evaluation was performed through the optimization stages of chitin conversion to chitosan, modifying the structure into beads and derivatives of chitosan, and subsequent adsorption-desorption processing using SPE techniques. Results showcase that a further increase in the degree of deacetylation (DD) of chitosan, as well as the chitosan conversion to its derivatives with covalent and electrostatic ionic bonds, significantly boosts the selectivity and capture capability towards Ni(II) and Zn(II) metals. Chitosan bead adsorbent derivatives KGb and KTb maintain high calculated adsorption, especially when pH is within the range of 5-6, and at low pH due to other newly formed active sites resulting from deprotonation, sustaining their effectiveness. As proposed, bonding is primarily chemical, following the Langmuir isotherm, and as for the governing interphase, both soft and hard base-acid characters influence the process. The set SPE technique effectively showed the ability to enrich Ni(II) and Zn(II) metals from concentration levels of µg/L to mg/L, proving promise to serve as a method for the preconcentration of trace metals. In the future, research can aim at improving the structural stability of the adsorbents in actual oceanic conditions, designing SPE-based continuous column systems, and studying field-scale reuse and regeneration of the adsorbents to promote ecologically safe seawater and industrial wastewater treatment.

ACKNOWLEDGMENTS

The authors gratefully acknowledge the facilities support from the Faculty of Teacher Training and Education, Iqra Buru University, and the Faculty of Mathematics and Natural Sciences, Universitas Gadjah Mada.

CONFLICT OF INTERESTS

The authors report no conflicts of interest.

AUTHOR CONTRIBUTIONS

The present work is related to *SDG-14: Life Below Water*. All the authors contributed significantly to this manuscript, participated in reviewing/editing and approved the final draft for publication. The research profile of the authors can be verified from their ORCID ids, given below:

M. Sehol https://orcid.org/0009-0001-7725-0847
K. Kasmawati https://orcid.org/0000-0002-0134-5823
N. Narsito http://orchid.org/0000-0002-5982-8983
S.J. Santosa https://orcid.org/0000-0002-6627-6806
J. Jumina https://orcid.org/0000-0003-2604-7838
R. Sholehah hhttps://orcid.org/0009-0000-3042-7863
Z.D. Firdaus https://orcid.org/0009-0000-7258-5034
M. Mahfud https://orcid.org/0000-0001-7740-9670
M.A. Ardiputra http://orchid.org/0009-0007-7244-6115
B. Sardi http://orchid.org/0000-0001-9555-0301

REFERENCES

1. M.M.M. Abbas, A.A. El-Kady, M.H. Ghanem, M.A. Embaby, M.A. El-Shorbagy, D.F.I. Ahmed, S. M. Abdel-Moniem, *Egyptian Journal of Aquatic Biology and Fisheries*, **28**, 1331(2024), https://doi.org/10.21608/ejabf.2024.396343.
2. B.H. Abdelmonem, L.T. Kamal, R.M. Elbaz, M.R. Khalifa, A. Abdelnaser, *Heliyon*, **11**, e41713(2025), https://doi.org/10.1016/j.heliyon.2025.e41713.
3. A. Sumaila, M.M. Ndamitso, Y.A. Iyaka, A.S. Abdulkareem, J.O. Tijani, M.O. Idris, *Iraqi Journal of Science*, **61**, 2156(2020), https://doi.org/10.24996/ijs.2020.61.9.2.

4. Z.A. Sutirman, M.M. Sanagi, K.J. Abd Karim, A.A.Naim, W.A.W. Ibrahim, *Malaysian Journal of Analytical Sciences*, **22**, 839(2018), https://doi.org/10.17576/mjas-2018-2205-11.
5. T.K. Dhaniswara, B. Sardi, S.R. Juliastuti, M. Mahfud, *Cleaner Waste Systems*, **11**, 100305(2025), https://doi.org/10.1016/j.clwas.2025.100305.
6. K. Khairuddin, M.A. Ridhawansa, R. Ruslan, B. Sardi, *Cleaner Waste Systems*, **10**, 100225(2025), https://doi.org/10.1016/j.clwas.2025.100225.
7. M. Mahfud, A.H. Ramadhana, N.A. Novita, F. Kurniawansyah, B. Sardi, M.Mirzan, L. Mahmudin, A.A. Ali, N. Indrawan, *Energy*, **341**, 134309(2024), https://doi.org/10.1016/j.energy.2024.134309.
8. O.F. Asokogene, M.A.A. Zaini, M.M. Idris, S. Abdulsalam, A.E.N. Usman, *International Journal of Chemical Reactor Engineering*, **17**, 1(2019), https://doi.org/10.1515/ijcre-2018-0274.
9. W. Al-Gethami, M.A. Qamar, M. Shariq, A.N.M.A. Alaghaz, A. Farhan, A.A. Areshi, M.H. Alnasir, *RSC Advances*, **14**, 2804(2024), https://doi.org/10.1039/d3ra06501d.
10. B.T. Iber, D. Torsabo, C.E.N.C.E. Chik, F. Wahab, S.R.S. Abdullah, H.A. Hassan, N.A. Kasan, *Journal of Sea Research*, **190**, 102306(2022), https://doi.org/10.1016/j.seares.2022.102306.
11. C. Gonzalez-Valerio, A.A. Peregrina-Lucano, R. Manríquez-González, A.A. Pérez-Fonseca, J.R. Robledo-Ortíz, I.G. Shenderovich, S. Gómez-Salazar, *Molecules*, **29**, 1(2024), https://doi.org/10.3390/molecules29245910.
12. D.F. Fitriyana, R. Ismail, A.P. Bayuseno, S. Anis, B. Priwintoko, Y. Subagyo, J. Jamari, J.P. Siregar, T. Cionita, J. Jaafar, *Journal of Advanced Research in Fluid Mechanics and Thermal Sciences*, **120**, 56(2024), https://doi.org/10.37934/arfmts.120.2.5666.
13. Y. Lailun, H. Harmami, I. Ulfin, S. Suprapto, C.W. Saleh, *Malaysian Journal of Fundamental and Applied Sciences*, **15**, 159(2019), https://doi.org/10.11113/mjfas.v15n2.971.
14. B. Sardi, I. Uno, F.A. Marhum, A.A. Akbar, T. Arief, M. Arif, A. Altway, M. Mahfud, *International Journal of Hydrogen Energy*, **49**, 203(2024), https://doi.org/10.1016/j.ijhydene.2023.07.217.
15. M. Malik, K.H. Chan, G. Azimi, *RSC Advances*, **11,** 28014(2021), https://doi.org/10.1039/d1ra03962h.
16. N.A.H. Narudin, N.A. Rosman, E.W.E. Shahrin, N. Sofyan, A. Hanif Mahadi, E. Kusrini, J. Hobley, A. Usman, Extraction, *Polymers and Polymer Composites*, **30**, 1(2022), https://doi.org/10.1177/09673911221109611.
17. B. Tekın, Ü. Açikel, *Turkish Journal of Chemistry*, **46**, 1042(2022), https://doi.org/10.55730/1300-0527.3413.
18. P.B.B. Frenchibai, R. Vinayagam, D. Ambigapathi, G.K. Anbazhagan, L. Elumalai, S. Palaniyandi, N.S.G.S. Thangam, K. Dharmalingam, *Biomedical Materials & Devices*, (2025), https://doi.org/10.1007/s44174-025-00334-0.
19. F.S. Chang, H.Y. Chin, M.L. Tsai, *Research on Chemical Intermediates*, **44**, 4939(2018), https://doi.org/10.1007/s11164-018-3346-8.
20. A.K.da S. Oliveira, R. Rizzo, C.A.A.C. Silva, N.C. Ré, M.L. Caron, P.R. Fiorio, *AgriEngineering*, **6**, 4135(2024), https://doi.org/10.3390/agriengineering6040233.
21. A.B. Pires, L. Vitali, A. Tavares, C.A. Germano, S.M. Amorim, R.F.P.M. Moreira, R.A. Peralta, N. Neves, *Carbohydrate Polymers*, **256**, 117589(2021), https://doi.org/10.1016/j.carbpol.2020.117589.
22. K. Weerasinghe, S. Liyanage, U.R. Kumarasinghe, A.T. Cooray, *Polymers from Renewable Resources*, **13(3)**, 170(2022), https://doi.org/10.1177/2041247922112297 0.
23. T. Kim, J. Shin, B. An, *Polymers*, **15(2)**, 421(2023), https://doi.org/10.3390/polym15020421.
24. A.K. Mallik, S.F. Kabir, F.B.A. Rahman, M.N. Sakib, S.S. Efty, M.M. Rahman, *Journal of Environmental Chemical Engineering*, **10**, 108048(2022), https://doi.org/10.1016/j.jece.2022.108048.
25. R. Ruslan, B. Sardi, K. Khairuddin, N.K. Sumarni, W. Tiro, Z.P. Magfira, N. Ainun, M. Mahfud, *Journal of the Energy Institute*, **119**, 101942(2025), https://doi.org/10.1016/j.joei.2024.101942.

[RJC-9396/2025]